Removal of Dyes Using Graphene-Based Composites: a Review

Article *in* Water Air and Soil Pollution · April 2017

DOI: 10.1007/s11270-017-3361-1

CITATIONS
63

READS
2,284

5 authors, including:

Ishani Khurana
University of Delhi
11 PUBLICATIONS **157** CITATIONS
SEE PROFILE

Amit Saxena
44 PUBLICATIONS **567** CITATIONS
SEE PROFILE

Bharti ..
Research Institute
14 PUBLICATIONS **143** CITATIONS
SEE PROFILE

Jitender Khurana
University of Delhi
244 PUBLICATIONS **4,699** CITATIONS
SEE PROFILE

Some of the authors of this publication are also working on these related projects:

Synthesis of conjugates View project

reactions of nickel boride and Mg-MeOH View project

Water Air Soil Pollut (2017) 228:180
DOI 10.1007/s11270-017-3361-1

Removal of Dyes Using Graphene-Based Composites: a Review

Ishani Khurana · Amit Saxena · Bharti · Jitender M. Khurana · Pramod Kumar Rai

Received: 10 October 2016 / Accepted: 3 April 2017

Abstract Water contamination has reached an alarming state due to industrialization and urbanization and has become a worldwide issue. Dyes contaminate water and are addressed extensively by researchers. Various technologies and materials have been developed for the treatment of contaminated water. Among them, adsorption has attracted great attention due to its ease and cost-effective nature. In recent years, graphene-based composites have shown great potential for the removal of contaminants from water. The literature reveals the usefulness of composites of graphene with metal oxides, carbon derivatives, metal hybrids and polymers for the removal of organic dyes from contaminated water. In this review, efforts have been made to compile the studies on the removal of cationic and anionic dyes from water using graphene-based composites.

Keywords Adsorption · Composites · Contaminated water · Degradation · Dyes · Graphene

I. Khurana · A. Saxena · Bharti · P. K. Rai (✉)
Centre for Fire, Explosive and Environment Safety, DRDO, Timarpur, Delhi 110054, India
e-mail: pramrai@rediffmail.com

I. Khurana · J. M. Khurana
Department of Chemistry, University of Delhi, Delhi 110007, India

1 Introduction

Industrial and societal bodies have faced water challenges worldwide. Rapid industrialization and urbanization have resulted in significant increase in generation of wastewater which contains various toxicants such as dyes, heavy metals, chlorinated hydrocarbons, biological contaminants, explosives, radioactive nucleotides and toxic anions. Organic dyes, a common water pollutant, are used in textile, rubber, paper, plastic, food and printing industries. Dyes are mostly stable due to their complex molecular structure and, therefore, do not biodegrade readily. Synthetic dyes are usually toxic, carcinogenic and mutagenic and are stable to temperature, light and microbial attacks (Barka et al. 2011). Dyes enter the food chain through water bodies and cause adverse effects on both human and animal health (Mohanty et al. 2006). Around 15% of the dye is lost during the dyeing process; therefore, the removal of dyes from contaminated water has become an issue of significant importance worldwide (Houas et al. 2001). Researchers have reviewed the removal of dyes using adsorbents and environmental applications of graphene-based composites (Lü et al. 2012; Bharathi and Ramesh 2013).

Previously various techniques such as nanofiltration (Chakraborty et al. 2003), photodegradation (Kant et al. 2014), oxidation (Neamtu et al. 2004), biological treatment (El-Naas et al. 2009), adsorption (Idris et al. 2011) and liquid membrane separation (Daas and Hamdaoui 2010) have been developed for the degradation and removal of toxic dyes from contaminated water. Commercial activated carbon has been frequently

Published online: 12 April 2017

employed by dye manufacturing industries because of its high surface area and porosity for the removal of dyes (Carrott et al. 1991). In the last decade, various adsorbents derived from agricultural and solid wastes have also received extensive attention (Rehman et al. 2012).

Nanomaterials such as metal oxides, graphene and carbon nanotubes have given a new prospect to the pollutant management. Graphene, a one-atom-thick 2D layer sp^2-hybridized carbon, is the most intensively studied material in the world because of its exceptional electrical, mechanical, optical and chemical properties. Graphene has emerged as a useful nanoadsorbent for environmental applications because of its high theoretical surface area (~2620 m^2 g^{-1}) (Novoselov et al. 2004, 2012). Abundant oxygen-containing functional groups have been incorporated in graphene to get graphene oxide (GO) and reduced graphene oxide (RGO) (Haubner et al. 2010). GO is mainly synthesized by the Staudenmaier method (Yang et al. 2013a) and Hummers'/modified Hummers' method (Moradi et al. 2015). The presence of surface functionalities makes GO a promising material for environmental applications (Kemp et al. 2013; Zhao et al. 2011). The electrostatic interactions of the adsorbate with the graphene and GO make them the materials of choice for adsorption of charged species (Ramesha et al. 2011). Three-dimensional reduced graphene oxide macrostructures have been utilized for dye removal (Kim et al. 2015). Exfoliated graphene oxide (EGO) and RGO were used for the removal of orange G (OG) (Ramesha et al. 2011). The usage of either GO or RGO for effective adsorption depends on the charge on the dye.

The literature revealed that GO-based composites have been utilized for the removal of cationic and anionic dyes (Fig. 1). These composites with metal oxides, carbon derivatives, metal hybrids or polymers are synthesized mostly by solvo-thermal synthesis (Sun et al. 2011), hydrothermal process (Ghosh et al. 2013b), microwave-assisted route (Liu et al. 2013a), one-step sonochemical route (Chandra et al. 2012), coprecipitation (Deng et al. 2013) and ultrasonication route (Reddy et al. 2015). The recovery of adsorbent after use has always been a challenge; to overcome this, magnetically active graphene-based composites have been synthesized (Lu et al. 2013). The recent proliferation of research into graphene-based hybrid materials is due to their high surface area and high porosity. Therefore, efforts have been made in this review to compile the important studies on the removal of various classes of organic dyes from contaminated water using graphene-based composites.

2 Kinetic Models

In order to understand the mechanism of adsorption, various theoretical models have been applied on the reaction rate data, namely pseudo-first-order (Lagergren 1898), pseudo-second-order (Ho and Mckay 1999) and intraparticle diffusion kinetic models (Weber and Morris 1963). The kinetic parameters of dye adsorption onto the graphene-based composites are evaluated using these kinetic models.

The linear form of Lagergren's pseudo-first-order equation is as follows:

$$\log(q_e - q_t) = \log(q_e) - k_1 t \Big/ 2.303 \quad (1)$$

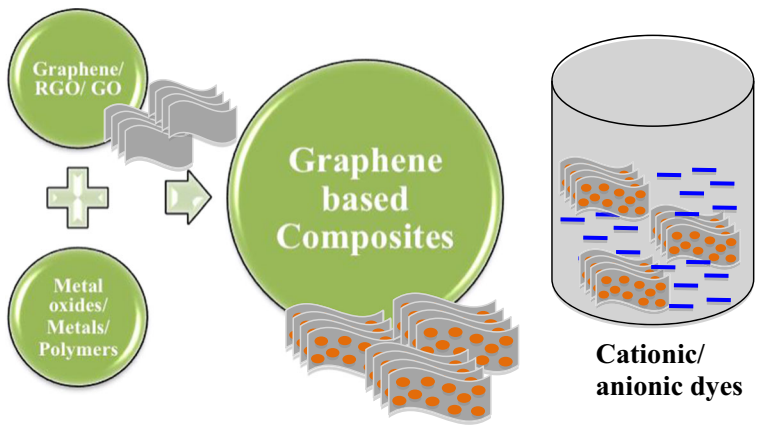

Fig. 1 Dye adsorption on graphene-based material

where q_e (mg g^{-1}) is the amount of adsorbed dye on the adsorbent at equilibrium, q_t (mg g^{-1}) is the amount of adsorbed dye on the adsorbent at time (t) and k_1 (min^{-1}) is the pseudo-first-order rate constant.

The linear form of pseudo-second-order equation is as follows:

$$\frac{t}{q_t} = \frac{1}{k_2\, q_e^2} + \frac{t}{q_e} \tag{2}$$

where q_e (mg g^{-1}) is the amount of adsorbed dye on the adsorbent at equilibrium, q_t (mg g^{-1}) is the amount of adsorbed dye on the adsorbent at time (t) and k_2 (g mg^{-1} min^{-1}) is the pseudo-second-order rate constant.

The model having a correlation coefficient (R^2) value closer to 1 for the linear regression plots and closer experimental and calculated q_e values is used for explaining the adsorption mechanism. In case, the pseudo-first-order model does not fit the experimental data well and then the pseudo-second-order model is used to explain the kinetics of the adsorption process. Literature reveals that generally, the adsorption kinetics for cationic and anionic dye removal by graphene-based nanocomposites follow the pseudo-second-order model (Rotte et al. 2014), although there are cases where the kinetics is well explained by the pseudo-first-order model (Wang et al. 2015a). Pseudo-second-order model assumes that chemisorption occurs; generally, the rate of direct adsorption/desorption process controls the sorption kinetics.

In order to understand the diffusion process of adsorptive onto the substrate, an intraparticle diffusion model proposed by Weber and Morris is utilized. Equation (3) represents the intraparticle diffusion.

$$q_t = k_i\, t^{0.5} + C \tag{3}$$

where q_t (mg g^{-1}) is the amount of adsorbed dye on the adsorbent at time (t), k_i (mg g^{-1} $min^{-0.5}$) is the intraparticle diffusion rate constant and C is constant.

The intraparticle diffusion model is used to understand the transport of adsorbate from the bulk solution phase to the surface pores of adsorbent. This gives the required information about the steps involved in the adsorption process. The adsorption mechanism is quite complex including the chemisorption and physisorption process when the value of C is not equal to zero. The adsorption kinetics is only controlled by intraparticle diffusion if $C = 0$. However, in most of the cases, the value for the constant (C) is non zero. Hence, the adsorption of dye onto the substrate is controlled by both film and intraparticle diffusions.

3 Adsorption Models

Adsorption models are helpful to understand the interactions between adsorptive molecules and adsorbents, and the distribution of these molecules between the liquid and solid phases at the equilibrium state. It plays an essential role in the optimization of the adsorbent usage for the selective removal of toxicants. The two majorly used models are Langmuir and Freundlich isotherm models. The best fit isotherm model is selected based on the value of correlation coefficient (R^2). The Langmuir adsorption is based on the assumption that a monolayer adsorption of adsorbate takes place over a homogeneous adsorbent surface. No transmigration of the adsorbate on the surface plane occurs.

The Langmuir isotherm is represented as

$$\frac{C_e}{Q_e} = \frac{1}{Q_M K_L} + \frac{C_e}{Q_M} \tag{4}$$

where C_e (mg L^{-1}) is the concentration of adsorptive at equilibrium, Q_e (mg g^{-1}) is the amount of adsorbed dye on the adsorbent at equilibrium, K_L (L mg^{-1}) is the Langmuir constant and Q_M (mg g^{-1}) is the Langmuir monolayer adsorption capacity.

The values of Q_M and K_L are calculated from the slope and intercept of the linear plot for the Langmuir model (C_e/q_e vs C_e).

The dimensionless separation factor (R_L) is used to describe the characteristics of Langmuir isotherm. It is represented as follows:

$$R_L = \frac{1}{1 + K_L C_o} \tag{5}$$

where C_o (mg L^{-1}) is the initial dye concentration, K_L (L mg^{-1}) is the Langmuir constant and R_L is the separation factor.

The possible R_L values explain whether the adsorption is favourable, unfavourable, linear or irreversible adsorption. If the value lies between 0 and 1, it represents favourable adsorption, $R_L > 1$ represents

unfavourable adsorption, $R_L = 1$ corresponds to linear adsorption and $R_L = 0$ represents irreversible adsorption.

The Freundlich adsorption isotherm model is based on the assumption that adsorbent surface is heterogeneous and multilayer adsorption takes place on its surface. The linear form of Freundlich adsorption isotherm model is as follows:

$$\log(Q_e) = \log(K_F) + \frac{1}{n}\log(C_e) \quad (6)$$

where Q_e (mg g^{-1}) is the equilibrium adsorption capacity of adsorbent, C_e (mg L^{-1}) is the equilibrium adsorptive concentration, K_F ($mg^{\left(1-\frac{1}{n}\right)} \cdot L^{\left(\frac{1}{n}\right)} \cdot g^{-1}$) is the Freundlich constants indicative of adsorption and $1/n$ is the Freundlich constants indicative of adsorption energy distribution.

The intercept and slope of the plot of log (Q_e) vs log (C_e) give the values of K_F and $1/n$. The values of $1/n$ between 0 and 1 indicate the adsorption intensity or surface heterogeneity. The value below 1 is indicative of normal Langmuir isotherm; however, the value above 1 corresponds to cooperative adsorption. As the heterogeneity increases, the value of $1/n$ tends to become 0.

Most of the dye removal has followed the Langmuir model (Fan et al. 2012; Ai et al. 2011; Deng et al. 2013; Li et al. 2013a, 2014; Yang et al. 2013a; Zhao et al. 2015a; Kim et al. 2015; Bian et al. 2013; Zhang et al. 2015) over the Freundlich model (Ai and Jiang 2012). However, a few authors have reported that adsorption follows both the Langmuir and Freundlich models (Ma et al. 2014).

4 Mechanism of Dye Removal

The removal is mostly carried out via either photodegradation or adsorption as depicted in Figs. 2 and 3, respectively. Ultra large surface area and strong π–π interaction on the surface of graphene composites are responsible for adsorption (Liu et al. 2012a). Along with the π–π interaction, the electrostatic interaction of oppositely charged functional groups on adsorbate and adsorbent leads to physical adsorption (Sharma and Das 2013; Tiwari et al. 2013). It has also been reported that the adsorption is strongly pH and ionic strength dependent, indicating an ion exchange mechanism (Fan et al. 2012). Better electrostatic interaction takes place between the negatively charged surface of GO sheets due

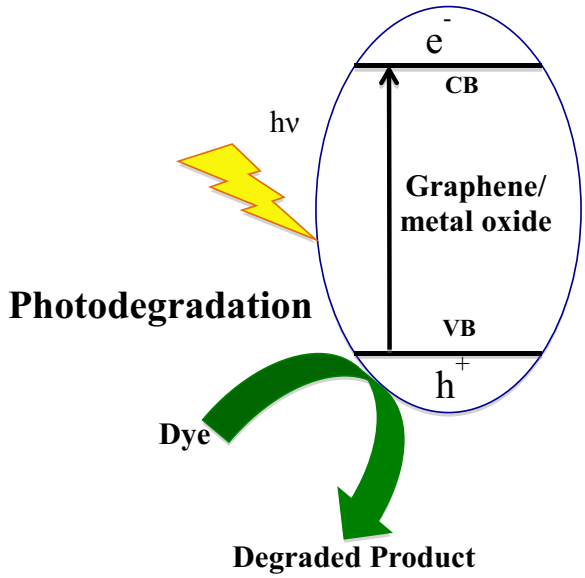

Fig. 2 Photodegradation mechanism of dyes using graphene/metal oxide composites

to the presence of oxygen functionalities and the positively charged cationic dyes (Ma et al. 2014). Therefore, some materials are more efficient for adsorption of cationic dyes over anionic dyes (Kim et al. 2015).

Besides adsorption, photodegradation or catalytic degradation of dyes has been carried out for rendering toxic dyes non-toxic. Chen et al. (2015) have discussed a general mechanism of photodegradation of organic dyes using β-Bi_2O_3-graphene composites. On irradiation of visible light, e^- in the valence band (VB) of β-Bi_2O_3 get excited to its CB, and as a result, holes (h^+) are generated in the VB of β-Bi_2O_3 simultaneously. As graphene is a good e^- acceptor and conductor, it promotes the effective separation of e^-–h^+ pairs which lead to swift transfer of the photogenerated electrons to the surface of graphene sheets. The photogenerated holes are available to react with OH^- to produce ·OH radicals. The holes that are generated in the VB of β-Bi_2O_3 are transferred to the VB of graphene. Hence, the lifetime of the holes increases, leading to the dye degradation process. These hydroxyl radicals are proposed to be the major active species responsible for the dye degradation. The photogenerated holes are the minor active species. The combined effect of the hydroxyl radicals and photogenerated holes leads to the oxidation of the organic dye pollutant to CO_2, H_2O and other small molecule compounds.

Zinc-based composites have also been widely used for dye degradation. RGO-ZnO is one such composite

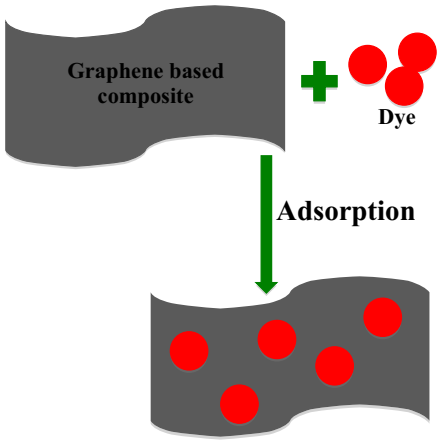

Fig. 3 Adsorption of dyes on high-surface-area graphene-based composites

used for the degradation of methylene blue dye (Luo et al. 2012). The photocatalytic activity of this composite on illumination of UV light is explained by the authors via formation of photogenerated charge pairs (e^-–h^+). The reaction of adsorbed O_2 and photogenerated electrons leads to the formation of $\cdot O_2^-$ and ·OH radicals, resulting into the photodegradation of the dye. The remaining holes in ZnO take part in the redox reactions in the photocatalytic process.

4.1 Removal of Cationic Dyes

4.1.1 Removal of Methylene Blue

Methylene blue (MB) is a cationic dye, which is used for dyeing silk, cotton and wool. MB poses harmful effects on human health such as diarrhoea, vomiting, increased heart rate, jaundice, quadriplegia, shock and cyanosis, and making its removal is necessary (Chen et al. 2011). MB can be removed from the contaminated water using various technologies and materials.

Carbon allotropes like activated carbon, GO, RGO and carbon nanotubes without any loadings have shown appreciable removal efficiencies against MB (Kim et al. 2015; Li et al. 2013a). Pristine carbon nanostructures (CNTs, RGO, carbon dots, activated carbon, etc.) have also been utilized for the removal of MB (Kim et al. 2015; Li et al. 2013a). Ramesha et al. (2011) have indicated 50% removal efficiency of RGO for cationic dyes. GO nanostructures (Liu et al. 2012a) and 3D RGO-based hydrogels (Tiwari et al. 2013) have also shown MB removal efficiencies to be 99.1 and 100%, respectively. The electrostatic attraction between graphite oxide and the dye was found to be responsible for the adsorption (Bradder et al. 2011). The kinetics of removal followed a pseudo-second-order model (Ma et al. 2014; Liu et al. 2012a). In order to enhance the sorption capacities of graphene, various composites of graphene have been prepared and studied for the efficient removal of MB (Table 1).

Zinc has been widely used to prepare composites with graphene. Zinc oxide nanorods indicated 66% photodegradation efficiency against MB, whereas its composite with RGO (RGO-ZnONR) indicated 99% efficiency (Nipane et al. 2015). A similar increase in degradation efficiencies was also observed with zinc oxide nanoparticles/RGO (ZnO-NPs/RGO) (Azarang et al. 2014) and RGO-hierarchical ZnO (RGO-ZnO) hollow sphere composites under UV (Luo et al. 2012). RGO-ZnO nanohybrids demonstrated superior photoactivity for the decolorization of self-photosensitized dyes under visible light (Liu et al. 2012b). Hybrid 3D structures composed of zinc oxide nanorods and reduced graphene oxide hydrogel were also reported for the removal of MB dye (Luan et al. 2015). Magnetic $ZnFe_2O_4$/graphene ($ZnFe_2O_4$/G) composite has shown dual function: first, as a catalyst for photoelectrochemical degradation of dyes, and second, as the generator of a strong oxidant hydroxyl radical via photoelectrochemical decomposition of H_2O_2 under visible light irradiation (Lu et al. 2013). $ZnFe_2O_4$/G composite indicated complete degradation of MB, and its excellent magnetic property has made it a magnetically recyclable material. Bi_2S_3-ZnS/graphene complexes could remove 50% MB (Liu et al. 2015). Yoon et al. (2015) synthesized graphene, charcoal, ZnO and ZnS/BiOX (X = Cl, Br and I) hybrid microspheres. Ten mole percent of ZnS or ZnO with BiOI was found to be the most promising composite for MB adsorption from mixed dye solutions.

Magnetic graphene composites, for facile recycling of the catalyst, have been utilized for the removal of MB. Graphene nanosheets (GNSs)/magnetite (Fe_3O_4) showed the adsorption capacity of ~15 mg g^{-1} (Ai et al. 2011), whereas Deng et al. (2013) showed the maximum sorption capacity as 64.23 mg g^{-1} using magnetic GO (MGO). The kinetics was well described by the pseudo-second-order model in both the cases (Ai et al. 2011; Deng et al. 2013). Mei et al. (2015) observed 71.6% degradation using MnO_2/G nanocomposite. Vinothkannan et al. (2015) showed that π–π stacking,

Table 1 Removal of methylene blue

Material	Dye concentration	Dosage	Activity	Reference
RGO-ZnONR	10 ppm	45 mg in 100 mL	Degradation of 99%	Nipane et al. (2015)
ZnO-NPs/RGO	10 mg mL^{-1}	10 mg in 30 mL	Degradation of 99.5%	Azarang et al. (2014)
$ZnFe_2O_4$/G	20 mg L^{-1}	50 mg in 50 mL	Degradation of 100%	Lu et al. (2013)
GNS/Fe_3O_4	10–25 mg L^{-1}	0.01 g in 25 mL	Adsorption capacity of ~15 mg g^{-1} (first cycle)	Ai et al. (2011)
MGO	90 mg L^{-1}	20 mg in 20 mL	Sorption of 64.23 mg g^{-1}	Deng et al. (2013)
MnO_2/G	65 mg L^{-1}	40 mg in 100 mL	Discoloration of 71.67%	Mei et al. (2015)
RGO/Fe_3O_4	9.37×10^{-5} M	10 mg	Complete degradation	Vinothkannan et al. (2015)
GO-$NiFe_2O_4$	20 mg L^{-1}	0.1 g in 50 mL	Decolorization of 96.2%	Liu et al. (2013b)
Mn_2O_3-G	4×10^{-6} M	2 mL (0.5 mg mL^{-1}) with H_2O_2	Degradation of ~84%	Chandra et al. (2012)
Bi_2O_3-RGO	5 mg L^{-1}	2 g L^{-1}	Degradation of 96%	Liu et al. (2013a)
NiO/GO	40 mg L^{-1}	20 mg	Removal efficiency of 97.54%	Rong et al. (2015b)
G-SnO_2	2.7×10^{-5} M	10 mg in 50 mL	Complete degradation	Seema et al. (2012)
CdSe-G	10–100 μmol L^{-1}	0.03 g	Removal: almost 100%	Chun et al. (2011)
GO-BiOBr	10 mg L^{-1}	50 mg in 100 mL	Degradation of 98%	Vadivel et al. (2014)
Au/graphene	10^{-5} M	50 μL and 0.5 mL ($NaBH_4$, 0.1 M) in 2.5 mL	17,000 times faster rate of reduction than un-catalyzed reaction	Siddhardha et al. (2014)
Noble metal-loaded graphene	0.1 mg mL^{-1}	10 mg in 100 mL	–	Ullah et al. (2014)
RGO/PAM	50–250 mg L^{-1}	–	Adsorption capacity of 1530 mg g^{-1}	Yang et al. (2013a)
SG-PVA	80.0 mg L^{-1}	2.0 g in 25 mL	Adsorption capacity of 13.54 mg g^{-1}	Li et al. (2015)
β-CD/PAA/GO	5–200 mg L^{-1}	4 mg in 6 mL	Adsorption capacity of 247.99 mg g^{-1}	Liu et al. (2014)

hydrogen bonding and electrostatic interactions were responsible for the easy adsorption and, subsequently, complete degradation of MB on RGO–Fe_3O_4 nanocomposite. GO-doped $NiFe_2O_4$ (GO-$NiFe_2O_4$) composite used as photo-Fenton catalyst in the presence of oxalic acid under visible light irradiation that could degrade >96% of MB (Liu et al. 2013b), whereas bare $NiFe_2O_4$ with H_2O_2 failed to degrade the dye.

Mn_2O_3-decorated graphene (Mn_2O_3-G) nanosheets have been reported as an effective heterogeneous catalyst for the photodegradation of organic dyes (Chandra et al. 2012). It exhibited 84% degradation of MB under UV irradiation. Bi_2O_3-reduced graphene oxide (Bi_2O_3-RGO, 2 wt%) composite achieved 96% MB degradation efficiency that was only 76% for Bi_2O_3 (Liu et al. 2013a). Chen et al. (2015) suggested that hydroxyl radicals are the major active species responsible for the degradation of MB on β-Bi_2O_3-graphene nanocomposites. In P25–graphene (P25-GN) nanocomposite, as the graphene content was increased, visible light absorption intensity and specific surface area also increased, and the removal efficiency reached above 90% (Li et al. 2013b). Rong et al. (2015b) indicated 97.54% removal efficiency due to the synergistic adsorption and photodegradation of MB on NiO/GO composite. Graphene oxide–TiO_2 (GO-TiO_2) and graphene–carbon nanotube–TiO_2 (G-CNT-TiO_2) composites have also been employed for degradation of MB (Filice et al. 2016; Wang et al. 2014b).

Graphene–SnO_2 (G-SnO_2) and graphene–CdSe (CdSe-G) composites exhibited complete photocatalytic degradation of MB (Seema et al. 2012; Chun et al. 2011). GO-BiOBr (5%) composite showed 98% degradation of MB in 30 min (Vadivel et al. 2014). Sodium deoxycholate/graphene oxide (NaDC/GO) composite hydrogels were also reported for MB removal (Wang et al. 2015c). Siddhardha et al. (2014) increased the MB degradation activity of Au (nanoparticles)/graphene up to 17,000 times than un-catalyzed reaction. Ullah et al. (2014) synthesized noble metal-loaded graphene hybrids, among which the Pt/graphene nanocomposites showed enhanced photocatalytic activities.

Polymer composites of RGO and GO have also shown better dye removal properties than their counter parts. RGO/polyacrylamide (RGO/PAM) (Yang et al. 2013a) and sulfonated graphene-enhanced polyvinyl alcohol (SG-PVA) hydrogel (Li et al. 2015) followed the pseudo-second-order kinetics model with adsorption capacity of 1530 and 13.54 mg g^{-1}, respectively. Liu et al. (2014) prepared β-cyclodextrin/poly(acrylic acid)/GO (β-CD/PAA/GO) nanocomposite exhibited excellent water dispersibility due to hydrophilic nature and observed maximum adsorption capacity of 247.99 mg g^{-1} against MB.

4.1.2 Removal of Rhodamine Blue

Rhodamine dyes are generally toxic and are soluble in water, methanol and ethanol. Rhodamine blue (RhB) is harmful to human and aquatic life. GO, graphite oxide, thermally reduced graphite oxide and exfoliated graphene oxide alone have shown promising results for the removal of RhB (Ramesha et al. 2011; Guardia et al. 2012; Avetta et al. 2015). Researchers have also explored numerous graphene-based composites for the removal of RhB (Table 2).

Pillaring chemically exfoliated graphene oxide with carbon nanotubes has been used as visible light photocatalyst against RhB (Zhang et al. 2010). Reduced graphene oxide-based hydrogels exhibited removal capability of 97% for RhB (Tiwari et al. 2013).

The magnetic $ZnFe_2O_4$/G composite showed excellent visible-light photocatalytic activity for the complete degradation of RhB in the presence of H_2O_2 (Lu et al. 2013). RGO-ZnO composite exhibited an exceptional cyclic performance against RhB with 99% catalyst recovery over several cycles under simulated sunlight irradiation (Wang et al. 2012). A novel Bi_2S_3-ZnS/G complex degraded RhB concentrations to 60% of the initial amount (Liu et al. 2015). Graphene, charcoal, ZnO and ZnS/BiOX (X = Cl, Br and I) hybrid microspheres have been used for the removal of mixture of dyes including RhB (Yoon et al. 2015). RGO-ZnO nanohybrid prepared by a microwave-assisted route demonstrated enhanced photoactivity leading to degradation of RhB, under visible light (Liu et al. 2012b).

Metal-loaded graphene was prepared for the removal of RhB. Siddhardha et al. (2014) reported that degradation rate of RhB by the Au (nanoparticle)/graphene composite was almost two times faster than that of citrate-capped Au nanoparticles of similar size. A synergistic interplay of pristine gold's electronic relay and π–π stacking of graphene with the dye accounts for its superior activity. The Pt/graphene nanocomposites showed improved photocatalytic activity than bare graphene against RhB (Ullah et al. 2014). Ghosh et al. (2013b) reported 98% RhB degradation in the dark using CdSe-G. CdSe-G prepared in conjunction with

Table 2 Removal of rhodamine blue

Material	Dye concentration	Dosage	Activity	Reference
$ZnFe_2O_4$/G	20 mg L^{-1}	50 mg	Degradation: 100%	Lu et al. (2013)
RGO-ZnO	10 mg L^{-1}	12.5 mg in 100 mL	–	Liu et al. (2012b)
Au/graphene	10^{-5} M	50 μL in 2.5 mL	170-fold faster reduction than un-catalyzed reaction	Siddhardha et al. (2014)
Noble metal-loaded graphene	0.1 mg mL^{-1}	10 mg in 100 mL	–	Ullah et al. (2014)
CdSe-G	1×10^{-4} mol L^{-1}	1 g in 100 mL	Removal of 98% (in the dark)	Ghosh et al. (2013b)
CdSe-G-TiO_2	1×10^{-4} mol L^{-1}	0.5 g in 50 mL	Percentage degradation of 85%	Ghosh et al. (2013a)
Ag_3PO_4/GO	20 ppm	0.08 g in 80 mL	Complete degradation	Chen et al. (2013)
Ag-I/RGO	10 mg L^{-1}	100 mg in 100 mL	Catalytic efficiency of~96%	Reddy et al. (2015)
GO/Ag_3PO_4	10 mg L^{-1}	0.075 g in 75 mL	–	Wang et al. (2014a)
MRGO	0.5–4 mg L^{-1}	0.234 g L^{-1}	Removal efficiency of over 91%	Sun et al. 2011
Ternary P25–graphene–Fe_3O_4	5 mg L^{-1}	10 mg in 50 mL	–	Cheng et al. (2016)
G/ZrO_2	10 mg mL^{-1}	50 mg mL^{-1} in 50 mL	–	Singh et al. (2015)
Mn_2O_3-G	1.2×10^{-5} M	0.5 mg mL^{-1} (in H_2O_2)	Degradation of ~60%	Chandra et al. (2012)
β-$SnWO_4$-RGO	1×10^{-4} M in 100 mL DD water	4 mg mL^{-1}	Photocatalytic degradation efficiency of 91%	Thangavel et al. (2014)
SnS_2/RGO	40–600 mg L^{-1}	2 mg mL^{-1} in 10 mL	Adsorption capacity of 94.07 mg g^{-1}	Bian et al. (2013)
GO-BiOBr	10 mg L^{-1}	50 mg in 100 mL	Removal efficiency of 95%	Vadivel et al. (2014)
CuI-RGO	20 mg L^{-1}	100 mg in 100 mL	Photocatalytic adsorption capacity of 2 mg mL^{-1}	Choi et al. (2015)
Carboxy-GO-zeolite	1–500 mg dm^{-3}	0.01 g	Adsorption capacity of 67.56 mg g^{-1}	Yu et al. (2013)
3D GO–polyethylenimine	50 mg L^{-1}	10 mg in 200 mL	–	Sui et al. (2013)

TiO_2 (CdSe-G-TiO_2) could degrade 85% RhB (Ghosh et al. 2013a). These composites exhibited impressive recyclability and stability. Chen et al. (2013) synthesized Ag_3PO_4/GO via a liquid-phase deposition method and reported complete degradation of RhB. The author showed that photocatalytic performance of Ag_3PO_4/GO was enhanced due to the improved adsorption performance and separation efficiency of photogenerated carriers. Ag-I/RGO nanocomposite indicated 96% catalytic activity against RhB (Reddy et al. 2015). The photocatalytic performance of GO/Ag_3PO_4 was greatly enhanced after incorporating GO (Wang et al. 2014a).

Researchers prepared magnetically active graphene hybrids because of their facile removal and reusability (Zhao et al. 2015b). Magnetite/reduced graphene oxide (MRGO) nanocomposites showed over 91% removal of RhB (Sun et al. 2011). Ternary P25–graphene–Fe_3O_4 nanocomposite has also been explored for the removal of RhB (Cheng et al. 2016).

Singh et al. (2015) reported green one-step alkaline synthesis of strongly bonded G-ZrO_2 nanocomposite and removal of 10 ppm RhB. Mn_2O_3-G nanosheets were synthesized by a simultaneous reduction of potassium permanganate along with GO, in which metal ions were first anchored through binding with oxy-functional groups of GO and finally reduced by hydrazine (Chandra et al. 2012). This composite could degrade 60% RhB under UV irradiation. β-$SnWO_4$-RGO nanocomposites were reported to degrade 91% RhB (Thangavel et al. 2014). SnS_2 nanoflakes along with a small amount of SnS_2 decorated on RGO sheets (SnS_2/RGO) indicated an adsorption capacity of 94.07 mg g^{-1} (Bian et al. 2013).

The degradation efficiency of GO–5% BiOBr composite towards RhB was reported to be 95% (Vadivel et al. 2014). CuI-RGO quasi-shell–core nanocomposites improved photocatalytic activities and stabilities for photodegradation of RhB under stimulated solar light irradiation (Choi et al. 2015). The benzene carboxylic acid derivatized GO-zeolite showed the maximum adsorption capacities of 67.56 mg g^{-1}. The kinetics followed the pseudo-second-order reaction model. GO nanosheets were also grafted to acid-treated natural clinoptilolite-rich zeolite powders followed by a coupling reaction with a diazonium salt (4-carboxybenzenediazoniumtetrafluoroborate) to the surface of GO (Yu et al. 2013). Adsorption capacity of the composite (carboxy-GO-zeolite) was found to be 67.56 mg g^{-1}, which was higher than pristine natural zeolite and GO-zeolite powders. Three-dimensional GO–polyethylenimine porous materials are also active for the removal of 50 ppm RhB (Sui et al. 2013).

4.1.3 Removal of Other Cationic Dyes

Carbon materials are extensively used for the removal of cationic dyes such as methyl violet (MV) (Ramesha et al. 2011; Liu et al. 2012a), methyl green (MeG) (Sharma and Das 2013), cationic light yellow 7GL (CLY 7GL) (Yang et al. 2013b), malachite green (MG) (Bradder et al. 2011; Suresh et al. 2015a, b; Ahmad et al. 2014), acridine orange (AcO) (Sun et al. 2012), new fuchsin dye (Roushani et al. 2015) and basic red 12 and basic red 46 (Moradi et al. 2015). Endothermic chemical adsorption through strong π–π stacking and anion–cation interaction accounts for adsorption (Liu et al. 2012a). Graphite oxide could remove 351 mg g^{-1} of MG via electrostatic attraction (Bradder et al. 2011). Adsorption capacity for AcO was reported to be 3.3 g g^{-1} (Sun et al. 2012). The adsorption capacity of RGO nanosheets against MeG increased while increasing the pH of the medium due to the change in the surface properties (Sharma et al. 2014). The presence of other ions like Na^+, Ca^{2+}, Mg^{2+} and SO_4^{2-} also influenced the adsorption property due to the change in the surface properties. Adsorption capacity in the presence of Na^+, Ca^{2+} and Mg^{2+} was 1.616, 1.562 and 1.436 mmol g^{-1}, respectively. The dye removal efficiencies have been improvised by synthesizing composites of graphene (Table 3).

MRGO nanocomposite indicated a maximum MG removal efficiency of >94%, and the removal was found to be dependent on the loading percentage of Fe_3O_4 and pH value (Sun et al. 2011). Li et al. (2015) used sulfonated graphene-enhanced polyvinyl alcohol (SP-PVA) composite hydrogel for the removal of MG and found that the kinetic data best fitted the pseudo-second-order kinetics model. The authors declared that SP hydrogels could be used for selective adsorption and separation of the dye mixtures. GO-doped $NiFe_2O_4$ (GO-$NiFe_2O_4$) was utilized as a photo-Fenton catalyst and was found to be capable of catalyzing the degradation of MG under visible light irradiation and in the presence of oxalic acid (Liu et al. 2013b).

Graphene oxide/cellulose bead has been reported as a facile and cost-effective adsorbent with removal efficiency of >96% against MG (Zhang et al. 2015). Wang et al. (2013) synthesized magnetic-sulfonic

Table 3 Removal of other cationic dyes

Dye	Material	Dye concentration	Dosage	Activity	Reference
MG	MRGO	0.5–4 mg L^{-1}	0.234 g L^{-1}	Removal efficiency of over 94%	Sun et al. (2011)
MG	SP-PVA	80.0 mg L^{-1}	2.0 g in 25 mL	–	Li et al. (2015)
MG	GO-$NiFe_2O_4$	20 mg L^{-1}	0.1 g in 50 mL	–	Liu et al. (2013b)
NR	G-SO_3H/Fe_3O_4	–	–	Adsorption capacity of 216.8 mg g^{-1}	Wang et al. (2013)
NR	Chi/nGO	0.025–7 mM	5 mg in 5 mL	Adsorption capacity of 57 × 10^{-2} mmol g^{-1}	González et al. (2015)
ST	β-CD/PAA/GO	5 to 200 mg L^{-1}	4 mg in 6 mL	Adsorption capacity of 175.49 mg g^{-1}	Liu et al. (2014)
MV	GPM	2000 mg L^{-1}	5 mg	Adsorption capacity of >2540 mg g^{-1}	Diagboya et al. (2014)
PA	G/Fe_3O_4	20–60 mg L^{-1}	4–10 mg in 20 mL	Adsorption capacity of 192.23 mg g^{-1}	Wu et al. (2013)
SO	MgO-G	4.0–5.0 × 10^{-4} M	0.05 g in 50 mL	Adsorption capacity of ~3.92 × 10^{-4} mol g^{-1}	Rotte et al. (2014)

graphene nanocomposite (G-SO_3H/Fe_3O_4) and explored its potential for the removal of Safranin T (ST), neutral red (NR) and victoria blue. Results revealed there was preferential adsorption of cationic dyes over anionic dyes at pH 6.0. Adsorption kinetics followed the pseudo-second-order kinetic model with maximum adsorption capacity as 216.8 mg g^{-1} for NR. Chitin/graphene oxide (Chi/nGO) hybrid gels indicated 57 × 10^{-2} mmol g^{-1} adsorption capacity against NR dye that was only 9.3 × 10^{-2} mmol g^{-1} for chitin (González et al. 2015). Water-soluble β-cyclodextrin/poly(acrylic acid)/graphene oxide nanocomposites has been used promisingly up to 5 cycles with 175.49 mg g^{-1} adsorption capacity against ST (Liu et al. 2014). Graphene oxide–tripolyphosphate hybrid (GPM) showed superior results for the adsorption of cationic dyes than anionic dyes (Diagboya et al. 2014). The adsorption was through electrostatic and π–π interactions, and the maximum adsorption capacity was found to be >2540 mg g^{-1} for cationic dyes. The pH and ionic strength played a major role in the adsorption of methyl blue on magnetic chitosan grafted with graphene oxide (Fan et al. 2012). The adsorption process followed an ion exchange mechanism with maximum adsorption capacity as >90%. Pararosaniline (PA) has been absorbed by superparamagnetic graphene–Fe_3O_4 (G/Fe_3O_4) nanocomposite (Wu et al. 2013). Multilayered MgO-decked graphene (MgO-G) indicated adsorption capacity as 3.92 × 10^{-4} mol g^{-1} against Safranin O (SO) and followed a pseudo-second-order rate equation (Rotte et al. 2014).

4.2 Removal of Anionic Dyes

4.2.1 Removal of Methyl Orange

Methyl orange (MO) is highly toxic due to mutagenic properties. It may be fatal if it is swallowed, inhaled or adsorbed through the skin. A variety of materials has been evaluated for the treatment of anionic dye in contaminated water. The selection of RGO and GO for effective adsorption can be ascribed to the charge on the dye, and the maximum removal efficiency of 95% was achieved using RGO against anionic dyes (Ramesha et al. 2011).

Table 4 shows graphene-based composites employed for the removal of MO. Zinc with graphene is extensively used to remove anionic dyes; e.g. RGO with zinc oxide has been used for the photodegradation of MO (Nipane et al. 2015; Zhang et al. 2013). The degradation efficiency increased from 25 to 78% on clubbing ZnO with RGO (Zhang et al. 2013). Lu et al. (2013) reported 96% photocatalytic degradation of MO using a magnetic $ZnFe_2O_4$/G composite in the presence of H_2O_2 under visible light. Graphene, charcoal, ZnO and ZnS/BiOX (X = Cl, Br and I) hybrid microspheres showed potential application for degradation of MO (Yoon et al. 2015). The order of degradation of the dye changed from RhB < MB < MO to MB < RhB < MO while using ZnO/BiOI and ZnS/BiOI. A BiOI-based catalyst was found to be superior to BiOCl and BiOBr. RGO-ZnCdS supramolecular photocatalyst has also been utilized to photocatalytically degrade 10^{-5} mol L^{-1} MO (Shen et al. 2015).

Table 4 Removal of methyl orange

Material	Dye concentration	Dosage	Activity	Reference
RGO-ZnONR	10 ppm	45 mg in 100 mL	Degradation efficiency of 78%	Nipane et al. (2015)
RGO-ZnO	10 ppm	30 mg in 120 mL	–	Zhang et al. (2013)
$ZnFe_2O_4$/G	20 mg L^{-1}	50 mg in 50 mL	Degradation of 96%	Lu et al. (2013)
CdSe-G	100 to 10 μmol L^{-1}	0.03 g	Removal of 6%	Chun et al. (2011)
CdSe-G	1×10^{-4} mol L^{-1}	1 g in 100 mL	Degradation efficiency of 90% (in the dark)	Ghosh et al. (2013b)
CdSe-G-TiO_2	1×10^{-4} mol L^{-1}	0.5 g in 50 mL	Percentage degradation of 71%	Ghosh et al. (2013a)
Ag_3PO_4/GO	20 ppm	0.08 g in 80 mL	Degradation ratio of ~86.7%	Chen et al. (2013)
TiO_2/G	0.02 g L^{-1}	80 mg in 100 mL	Decomposition of >75%	Han et al. (2015)
3D G-TiO_2	20 mg L^{-1}	10 mg in 40 mL	–	Zhao et al. (2015a)
β-$SnWO_4$-RGO	1×10^{-4} M in 100 mL DD water	4 mg mL^{-1}	Photocatalytic degradation efficiency of 90%	Thangavel et al. (2014)
Bi_2O_3-RGO	5 mg L^{-1}	2 g L^{-1} in 80 mL	Degradation rate of 93%	Liu et al. (2013a)
Cu_2O/GO/chitin	10 mg L^{-1}	–	Degradation of 92.1%	Wang et al. (2015b)
Cu_2O/PA/RGO	30 mg L^{-1}	10 mg in 20 mL	Photocatalytic degradation of 95%	Yan et al. (2013)

CdSe-G composites have been reported for dye removal (Chun et al. 2011; Ghosh et al. 2013a, b). Chun et al. (2011) indicated only 6% MO removal, whereas Ghosh et al. (2013b) reported 90% degradation (in the dark) using CdSe-G under different experimental conditions. A comparative study was carried out to investigate the synergistic effect of graphene on CdSe and TiO_2 (Ghosh et al. 2013a). CdSe–graphene–TiO_2 (CdSe-G-TiO_2) composite degraded 71% of MO. Chen et al. (2013) achieved 86.7% degradation of MO using Ag_3PO_4/GO composite and indicated that adsorption performance and separation efficiency of photogenerated carriers were accounted for the enhanced photocatalytic performance. Torres et al. (2013) indicated improved performance of GO-P25 due to the reduction of GO during thermal treatment, which led to the good contact between TiO_2 and carbon phases. Flocculent-like TiO_2/G has been reported for the decomposition of MO to the tune of >75% (Han et al. 2015). Zhao et al. (2015a) found that 3D G-TiO_2 nanotube composite provided both active sites and electron transport path for its photocatalytic activity against MO.

GO and titania hybrid Nafion membranes could remove 71% of MO (Filice et al. 2015). β-$SnWO_4$-RGO nanocomposite indicated excellent photocatalytic activity with degradation efficiency of 90% in a short time against MO (Thangavel et al. 2014). Bi_2O_3 with 2 wt% RGO achieved a maximum MO degradation efficiency of 93% (Liu et al. 2013a). Wang et al. (2015b) prepared a Cu_2O/GO/chitin composite film and observed improved photocatalytic activity due to the introduction of GO. The degradation efficiency against 10, 25 and 50 ppm of MO was 92.1, 72.3 and 48.3%, respectively, within 3 h. Yan et al. (2013) also reported the photocatalytic degradation of MO up to 95% using Cu_2O/*n*-propylamine (PA)/RGO composite.

4.2.2 Removal of Other Anionic Dyes

Other anionic dyes besides MO have also been removed by bare GO, RGO, etc. Kim et al. (2015) evaluated a 3D RGO macrostructure alone for the adsorption of acid red 1 and obtained the maximum adsorption capacity of 277.01 mg g^{-1}. Authors also found that the studies followed the pseudo-second-order kinetics and Freundlich models. Ramesha et al. (2011) used EGO and RGO for the removal of OG.

Degradation of various other anionic dyes by graphene-based composites is summarized in Table 5.

Table 5 Removal of other anionic dyes

Dye	Material	Dye concentration	Dosage	Activity	Reference
FA	GO/chitosan	50–150 mg L^{-1}	10 mg in 20 mL	Adsorption capacity of 175.4 mg g^{-1}	Li et al. (2014)
OG	Magnetic GO	60 mg L^{-1}	20 mg in 20 mL	Adsorption capacity of 20.85 mg g^{-1}	Deng et al. (2013)
RB	Chi/nGO	0.025–5 mM	5 mg in 5 mL	Adsorption capacity of 57×10^{-2} mmol g^{-1}	González et al. (2015)
AM	3D GO–polyethylenimine	50 mg L^{-1}	10 mg in 200 mL	Adsorption capacity of 800 mg g^{-1}	Sui et al. (2013)
AO7	Pt-TiO_2/G	35 mg L^{-1}	10 mg in 60 mL	Degradation efficiency of 99%	Hsieh et al. (2015)
Eosin	Mn_2O_3-G	2.5×10^{-5} M	2 mL (0.5 mg mL^{-1}) in 50 mL with H_2O_2	Degradation: almost 80%	Chandra et al. (2012)
O II	Mn_3O_4-RGO	30–90 mg L^{-1}	10 mg and 0.3 g Oxone in 200 mL	Removal of 100% or 30 ppm	Yao et al. (2013)
O II	Co_3O_4/GO	0.2 mM	0.1 g L^{-1} with 1 mM Oxone	Degradation of 100%	Shi et al. (2012)
CR	NiO/GNS	20 mg L^{-1}	50 mg in 100 mL	Adsorption of 99.56%	Rong et al. (2015a)
PS	PDDA/GO	0.001–1 mM	1.0 mg in 500 μL	Adsorption capacity of 188.679 mg g^{-1}	Wang et al. (2014c)
TB	PDDA/GO	0.001–1 mM	1.0 mg in 500 μL	Adsorption capacity of 50.025 mg g^{-1}	Wang et al. (2014c)
O IV	3D G-Fe	200 mg L^{-1}	10 mg in 50 mL	Removal of 94.5%	Wang et al. (2015a)

Li et al. (2014) prepared GO/chitosan composite fibres and evaluated it against fuchsin acid (FA). The adsorption was spontaneous and exothermic and followed pseudo-second-order kinetics with 175.4 mg g^{-1} adsorption capacity. Deng et al. (2013) also applied the pseudo-second-order model on the removal of OG by magnetic GO nanocomposite and reported the sorption capacity of 20.85 mg g^{-1}. González et al. (2015) observed that the adsorption of Remazol black (RB) on chitin-GO (Chi/nGO) hybrid gels depends on pH and Chi/nGO proportion. Three-dimensional GO–polyethylenimine porous materials indicated high adsorption capacity (800 mg g^{-1}) against amaranth (AM) and found it promising for the removal of OG (Sui et al. 2013).

Hsieh et al. (2015) reported degradation of acid orange 7 (AO7) by Pt-TiO_2/G nanocomposites. Pt-TiO_2 served as a charge-generating centre while graphene worked as an electron acceptor and transporter in the composite. Wang et al. (2013) utilized magnetic G-SO_3H/Fe_3O_4 for the adsorption of MO, brilliant yellow and alizarin red, and the adsorption followed the pseudo-second-order kinetic model. GPM hybrid has been used for the removal of anionic dyes (MO, alizarin yellow and AM) (Diagboya et al. 2014). GPM showed higher potency for adsorption of cationic dyes as a consequence of π–π and electrostatic interactions. Chandra et al. (2012) removed eosin by Mn_2O_3-G nanosheets. Mn_3O_4-RGO nanohybrids showed 61 and 100% removal against 60 and 30 ppm of orange II (O II), respectively (Yao et al. 2013). Shi et al. (2012) also showed complete removal of O II using well-dispersed Co_3O_4 nanoparticles over GO. Rong et al. (2015a) revealed the removal of Congo red (CR) using NiO/GNS. The process was well explained by the pseudo-second-order kinetic model, and the equilibrium data were well fitted by the Redlich–Peterson model. The use of poly(diallyldimethylammonium chloride)/GO (PDDA/GO) hydrogels indicated excellent removal efficiencies for Ponceau S (PS) and trypan blue (TB) due to strong π–π stacking and electrostatic interactions (Wang et al. 2014c). Zerovalent iron nanoparticle-decorated 3D graphene (3D G-Fe) indicated 94.5% removal of orange IV (O IV) and followed pseudo-first-order degradation kinetics (Wang et al. 2015a). The removal was due to adsorption and redox reaction with activation energy of 39.2 kJ mol^{-1}.

5 Conclusion and Future Perspectives

Graphene and its hybrids have been widely utilized for the removal and degradation of toxicants from water. Attempts are being made to further enhance the activity of graphene by mixing/loading it with other materials, e.g. metal oxides, metals, clay, polymers and biological materials. Graphene-based composites have been studied extensively by numerous research groups for the removal of organic dyes from water due to their enhanced catalytic activities, reusability and facile recovery. Zinc-based graphene composites have been extensively utilized for the removal of both cationic and anionic dyes. Kinetics data fitted the pseudo-second-order model. These composites removed organic dyes mainly via adsorption, free radical mechanism, photodegradation and electrostatic and π–π interactions. Magnetically active composites of graphene are materials of interest due to the easy and cost-effective separation techniques. An ideal composite should have high activity, high surface area, easy recovery and excellent stability. During the documentation of this review, it was concluded that light needs to be shed on combining graphene-based systems with other existing water-purifying technologies to improve their efficiency and achieve superior water quality. Partnerships among fundamental science and engineering development are essentially required to improvise the efficacy of treatment technologies.

Acknowledgements The authors are thankful to the Director, CFEES, Delhi, for the valuable guidance.

References

Ahmad, M. A., Ahmad, N., & Bello, O. S. (2014). Adsorptive removal of malachite green dye using durian seed-based activated carbon. *Water Air & Soil Pollution, 225*, 2057.

Ai, L., & Jiang, J. (2012). Removal of methylene blue from aqueous solution with self-assembled cylindrical graphene-carbon nanotube hybrid. *Chemical Engineering Journal, 192*, 156–163.

Ai, L., Zhang, C., & Chena, Z. (2011). Removal of methylene blue from aqueous solution by a solvothermal-synthesized graphene/magnetite composite. *Journal of Hazardous Materials, 192*, 1515–1524.

Avetta, P., Sangermano, M., Lopez-Manchado, M., & Calza, P. (2015). Use of graphite oxide and/or thermally reduced graphite oxide for the removal of dyes from water. *Journal of Photochemistry and Photobiology A: Chemistry, 312*, 88–95.

Azarang, M., Shuhaimi, A., Yousefi, R., Golsheikh, A. M., & Sookhakian, M. (2014). Synthesis and characterization of ZnO NPs/reduced graphene oxide nanocomposites prepared in gelatine medium as highly efficient photo-degradation of MB. *Ceramics Internaional, 40*, 10217–10221.

Barka, N., Abennouri, M., El-Makhfouk, M., & Taiwan, J. (2011). Removal of methylene blue and Eriochrome Black T from aqueous solutions by biosorption on *Scolymushispanicus* L.: kinetics, equilibrium and thermodynamics. *Journal of the Taiwan Institute of Chemical Engineers, 42*(2), 320–326.

Bharathi, K. S., & Ramesh, S. T. (2013). Removal of dyes using agricultural waste as low-cost adsorbents: a review. *Applied Water Science, 3*, 773–790.

Bian, X., Lu, X., Xue, Y., Zhang, C., Kong, L., & Wang, C. (2013). A facile one-pot hydrothermal method to produce SnS_2/reduced graphene oxide with flake-on-sheet structures and their applicationin the removal of dyes from aqueous solution. *Journal of Colloid and Interface Science, 406*, 37–43.

Bradder, P., Ling, S. K., Wang, S., & Liu, S. (2011). Dye adsorption on layered graphite oxide. *Journal of Chemical & Engineering Data, 56*(1), 138–141.

Carrott, P. J. M., Carrott, M. M. L. R., & Roberts, R. A. (1991). Physical adsorption of gases by microporous carbons. *Colloids and Surfaces, 58*(4), 385–400.

Chakraborty, S., Purkait, M. K., Gupta, S. D., De, S., & Basu, J. K. (2003). Nanofiltration of textile plant effluent for color removal and reduction in COD. *Separation and Purification Technology, 31*(2), 141–151.

Chandra, S., Das, P., Bag, S., Bhar, R., & Pramanik, P. (2012). Mn_2O_3 decorated graphene nanosheet: an advanced material for the photocatalytic degradation of organic dyes. *Materials Science and Engineering B, 177*, 855–861.

Chen, L., Ramadan, A., Lv, L., Shao, W., Luo, F., & Chen, J. (2011). Biosorption of methylene blue from aqueous solution using lawny grass modified with citric acid. *Journal of Chemical & Engineering Data, 56*, 3392–3399.

Chen, G., Sun, M., Wei, Q., Zhang, Y., Zhu, B., & Du, B. (2013). Ag_3PO_4/graphene-oxide composite with remarkably enhanced visible-light-driven photocatalytic activity toward dyes in water. *Journal of Hazardous Materials, 244–245*, 86–93.

Chen, X., Dai, J., Shi, G., Li, L., Wang, G., & Yang, H. (2015). Visible light photocatalytic degradation of dyes by β-Bi_2O_3/graphene nanocomposites. *Journal of Alloys and Compounds, 649*, 872–877.

Cheng, L., Zhang, S., Wang, Y., Ding, G., & Jiao, Z. (2016). Ternary P25–graphene–Fe_3O_4 nanocomposite as a magnetically recyclable hybrid for photodegradation of dyes. *Materials Research Bulletin, 73*, 77–83.

Choi, J., Reddy, D. A., Islam, M. J., Seo, B., Joo, S. H., & Kim, T. K. (2015). Green synthesis of the reduced graphene oxide–CuI quasi-shell–core nanocomposite: a highly efficient and stable solar-light-induced catalyst for organic dye degradation in water. *Applied Surface Science, 358*(Part A), 159–167.

Chun, O. W., Mingliang, C., Kwangyoun, C., Cheolkyu, K., Zeda, M., & Lei, Z. (2011). Synthesis of graphene-CdSe composite by a simple hydrothermal method and its photocatalytic

degradation of organic dyes. *Chinese Journal of Catalysis, 32*, 1577–1583.

Daas, A., & Hamdaoui, O. (2010). Extraction of anionic dye from aqueous solutions by emulsion liquid membrane. *Journal of Hazardous Materials, 178*, 973–981.

Deng, J. H., Zhang, X. R., Zeng, G. M., Gong, J. L., Niu, Q. Y., & Liang, J. (2013). Simultaneous removal of Cd (II) and ionic dyes from aqueous solution using magnetic graphene oxide nanocomposite as an adsorbent. *Chemical Engineering Journal, 226*, 189–200.

Diagboya, P. N., Owolabi, B. I. O., Zhou, D., & Han, B. H. (2014). Graphene oxide–tripolyphosphate hybrid used as a potent sorbent for cationic dyes. *Carbon, 79*, 174–182.

El-Naas, M. H., Al-Muhtaseb, S. A., & Makhlouf, S. (2009). Biodegradation of phenol by *Pseudomonas putida* immobilized in polyvinyl alcohol (PVA) gel. *Journal of Hazardous Materials, 164*, 720–725.

Fan, L., Luo, C., Li, X., Lu, F., Qiu, H., & Sun, M. (2012). Fabrication of novel magnetic chitosan grafted with graphene oxide to enhance adsorption properties for methyl blue. *Journal of Hazardous Materials, 215–216*, 272–279.

Filice, S., D'Angelo, D., Libertino, S., Nicotera, I., Kosma, V., Privitera, V., & Scalese, S. (2015). Graphene oxide and titania hybrid Nafion membranes for efficient removal of methyl orange dye from water. *Carbon, 82*, 489–499.

Filice, S., D'Angelo, D., Spanò, S. F., Compagnini, G., Sinatra, M., D'Urso, L., Fazio, E., Privitera, V., & Scalese, S. (2016). Modification of graphene oxide and graphene oxide–TiO_2 solutions by pulsed laser irradiation for dye removal from water. *Materials Science in Semiconductor Processing, 42*, 50–53.

Ghosh, T., Cho, K. Y., Ullah, K., Nikam, V., Park, C. Y., Meng, Z. D., & Oh, W. C. (2013a). High photonic effect of organic degradation by CdSe–graphene–TiO_2 particles. *Journal of Industrial and Engineering Chemistry, 19*(3), 797–805.

Ghosh, T., Ullah, K., Nikam, V., Park, C. Y., Meng, Z. D., & Oh, W. C. (2013b). The characteristic study and sonocatalytic performance of CdSe–graphene ascatalyst in the degradation of azo dyes in aqueous solution under dark conditions. *Ultrasonics Sonochemistry, 20*, 768–776.

González, J. A., Villanueva, M. E., Piehl, L. L., & Copello, G. J. (2015). Development of a chitin/graphene oxide hybrid composite for the removal of pollutant dyes: adsorption and desorption study. *Chemical Engineering Journal, 280*, 41–48.

Guardia, L., Villar-Rodil, S., Paredes, J. I., Rozada, R., & Martínez-Alonso, A. & Tascón, J.M.D. (2012). UV light exposure of aqueous graphene oxide suspensions topromote their direct reduction, formation of graphene–metal nanoparticle hybrids and dye degradation. *Carbon, 50*, 1014–1024.

Han, W., Ren, L., Zhang, Z., Qi, X., Liu, Y., Huang, Z., & Zhong, J. (2015). Graphene-supported flocculent-like TiO_2 nanostructures for enhanced photoelectrochemical activity and photodegradation performance. *Ceramics International, 41*, 7471–7477.

Haubner, K., Murawski, J., Olk, P., Eng, L. M., Ziegler, C., Adolphi, B., & Jaehne, E. (2010). The route to functional graphene oxide. *Chem Phys Chem, 11*, 2131–2139.

Ho, Y. S., & Mckay, G. (1999). Pseudo-second order model for sorption processes. *Process Biochemistry, 34*, 451–465.

Houas, A., Lachheb, H., Ksibi, M., Elaloui, E., Guillard, C., & Herrmann, J. M. (2001). Photocatalytic degradation pathway of methylene blue in water. *Applied Catalysis B: Environmental, 31*(2), 145–157.

Hsieh, S. H., Chen, W. J., & Wu, C. T. (2015). Pt-TiO_2/graphene photocatalysts for degradation of AO7 dye under visible light. *Applied Surface Science, 340*, 9–17.

Idris, M. N., Ahmad, Z. A., & Ahmad, M. A. (2011). Adsorption equilibrium of malachite green dye onto rubber seed coat based activated carbon. *International Journal of Basic and Applied Sciences, 11*, 38–43.

Kant, S., Pathania, D., Singh, P., Dhiman, P., & Kumar, A. (2014). Removal of malachite green and methylene blue by $Fe_{0.01}Ni_{0.01}Zn_{0.98}O$/polyacrylamide nanocomposite using coupled adsorption and photocatalysis. *Applied Catalysis B: Environmental, 147*, 340–352.

Kemp, K. C., Seema, H., Saleh, M., Le, N. H., Mahesh, K., Chandra, V., & Kim, K. S. (2013). Environmental applications using graphene composites: water remediation and gas adsorption. *Nanoscale, 5*, 3149–3171.

Kim, H., Kang, S. O., Park, S., & Park, H. S. (2015). Adsorption isotherms and kinetics of cationic and anionic dyes on three-dimensional reduced graphene oxide macrostructure. *Journal of Industrial and Engineering Chemistry, 21*, 1191–1196.

Lagergren, S. (1898). About the theory of so-called adsorption of soluble substances. *Kungl Svenska Vetenskapsakademiens Handlingar, 24*, 1–39.

Li, Y., Du, Q., Liu, T., Peng, X., Wang, J., Sun, J., Wang, Y., Wu, S., Wang, Z., Xia, Y., & Xia, L. (2013a). Comparative study of methylene blue dye adsorption onto activated carbon, graphene oxide, and carbon nanotubes. *Chemical Engineering Research and Design, 91*(2), 361–368.

Li, J., Zhou, S. l., Hong, G. B., & Chang, C. T. (2013b). Hydrothermal preparation of P25–graphene composite with enhanced adsorption and photocatalytic degradation of dyes. *Chemical Engineering Journal, 219*, 486–491.

Li, Y., Sun, J., Du, Q., Zhang, L., Yang, X., Wu, S., Xia, Y., Wang, Z., Xia, L., & Cao, A. (2014). Mechanical and dye adsorption properties of graphene oxide/chitosan composite fibers prepared by wet spinning. *Carbohydrate Polymers, 102*, 755–761.

Li, H., Fan, J., Shi, Z., Lian, M., Tian, M., & Yin, J. (2015). Preparation and characterization of sulfonated graphene-enhanced poly (vinyl alcohol) composite hydrogel and its application as dye absorbent. *Polymer, 60*, 96–106.

Liu, F., Chung, S., Oh, G., & Seo, T. S. (2012a). Three-dimensional graphene oxide nanostructure for fast and efficient water-soluble dye removal. *ACS Applied Materials & Interfaces, 4*(2), 922–927.

Liu, Y., Hu, Y., Zhou, M., Qian, H., & Hu, X. (2012b). Microwave-assisted non-aqueous route to deposit well-dispersed ZnO nanocrystals on reduced graphene oxide sheets with improved photoactivity for the decolorization of dyes under visible light. *Applied Catalysis B: Environmental, 125*, 425–431.

Liu, X., Pan, L., Lv, T., Sun, Z., & Sun, C. Q. (2013a). Visible light photocatalytic degradation of dyes by bismuth oxide-reduced graphene oxide composites prepared via microwave-assisted method. *Journal of Colloid and Interface Science, 408*, 145–150.

Liu, S. Q., Xiao, B., Feng, L. R., Zhou, S. S., Chen, Z. G., Liu, C. B., Chen, F., Wu, Z. Y., Xu, N., Oh, W. C., & Meng, Z. D. (2013b). Graphene oxide enhances the Fenton-like photocatalytic activity of nickel ferrite for degradation of dyes under visible light irradiation. *Carbon, 64*, 197–206.

Liu, J., Liu, G., & Liu, W. (2014). Preparation of water-soluble β-cyclodextrin/poly(acrylic acid)/graphene oxide nanocomposites as new adsorbents to remove cationic dyes from aqueous solutions. *Chemical Engineering Journal, 257*, 299–308.

Liu, F., Shao, X., & Yang, S. (2015). Bi_2S_3–ZnS/graphene complexes: synthesis, characterization, and photoactivity for the decolorization of dyes under visible light. *Materials Science in Semiconductor Processing, 34*, 104–108.

Lü, K., Zhao, G., & Wang, X. K. (2012). A brief review of graphene-based material synthesis and its application in environmental pollution management. *Chinese Science Bulletin, 57*(11), 1223–1234.

Lu, D., Zhang, Y., Lin, S., Wang, L., & Wang, C. (2013). Synthesis of magnetic $ZnFe_2O_4$/graphene composite and its application in photocatalytic degradation of dyes. *Journal of Alloys and Compounds, 579*, 336–342.

Luan, V. H., Tien, H. N., & Hur, S. H. (2015). Fabrication of 3D structured ZnO nanorod/reduced graphene oxide hydrogels and their use for photo-enhanced organic dye removal. *Journal of Colloid and Interface Science, 437*, 181–186.

Luo, Q. P., Yu, X. Y., Lei, B. X., Chen, H. Y., Kuang, D. B., & Su, C. Y. (2012). Reduced graphene oxide-hierarchical ZnO hollow sphere composites with enhanced photocurrent and photocatalytic activity. *Journal of Physical Chemistry C, 116*(14), 8111–8117.

Ma, T., Chang, P. R., Zheng, P., Zhao, F., & Ma, X. (2014). Fabrication of ultra-light graphene-based gels and their adsorption of methylene blue. *Chemical Engineering Journal, 240*, 595–600.

Mei, J., Zhang, L., & Niu, Y. (2015). Fabrication of the magnetic manganese dioxide/graphene nanocomposite and its application in dye removal from the aqueous solution at room temperature. *Materials Research Bulletin, 70*, 82–86.

Mohanty, K., Naidu, J. T., Meikap, B. C., & Biswas, M. N. (2006). Removal of crystal violet from wastewater by activated carbons prepared from rice husk. *Industrial & Engineering Chemistry Research, 45*(14), 5165–5171.

Moradi, O., Gupta, V. K., Agarwal, S., Tyagi, I., Asif, M., Makhlouf, A. S. H., Sadegh, H., & Shahryari-ghoshekandi, R. (2015). Characteristics and electrical conductivity of graphene and graphene oxide for adsorption of cationic dyes from liquids: kinetic and thermodynamic study. *Journal of Industrial and Engineering Chemistry, 28*, 294–230.

Neamtu, M., Yedlier, A., Siminiceanu, I., Macoveanu, M., & Kellrup, A. (2004). Decolorization of disperse red 354 azo dye in water by several oxidation processes—a comparative study. *Dyes and Pigments, 60*(1), 61–68.

Nipane, S. V., Korake, P. V., & Gokavi, G. S. (2015). Graphene-zinc oxide nanorod nanocomposite as photocatalyst for enhanced degradation of dyes under UV light irradiation. *Ceramics International, 41*, 4549–4557.

Novoselov, K. S., Geim, A. K., Morozov, S. V., Jiang, D., Zhang, Y., Dubonos, S. V., Grigorieva, I. V., & Firsov, A. A. (2004). Electric field effect in atomically thin carbon films. *Science, 306*(5696), 666–669.

Novoselov, K. S., Fal'ko, V. I., Colombo, L., Gellert, P. R., Schwab, M. G., & Kim, K. (2012). A roadmap for graphene. *Nature, 490*, 192–200.

Ramesha, G. K., Kumara, A. V., Muralidhara, H. B., & Sampath, S. (2011). Graphene and graphene oxide as effective adsorbents toward anionic and cationic dyes. *Journal of Colloid and Interface Science, 361*(1), 270–277.

Reddy, D. A., Lee, S., Choi, J., Park, S., Ma, R., Yang, H., & Kim, T. K. (2015). Green synthesis of AgI-reduced graphene oxide nanocomposites: toward enhanced visible-light photocatalytic activity for organic dye removal. *Applied Surface Science, 341*, 175–184.

Rehman, M. S. U., Kim, I., & Han, J. I. (2012). Adsorption of methylene blue dye from aqueous solution by sugar extracted spent extracted spent rice biomass. *Carbohydrate Polymers, 90*, 1314–1322.

Rong, X., Qiu, F., Qin, J., Zhao, H., Yan, J., & Yang, D. (2015a). A facile hydrothermal synthesis, adsorption kinetics and isotherms to Congo red azo-dye from aqueous solution of NiO/graphene nanosheets adsorbent. *Journal of Industrial and Engineering Chemistry, 26*, 354–363.

Rong, X., Qiu, F., Zhang, C., Fu, L., Wang, Y., & Yang, D. (2015b). Adsorption-photodegradation synergetic removal of methylene blue from aqueous solution by NiO/graphene oxide nanocomposite. *Powder Technology, 275*, 322–328.

Rotte, N. K., Yerramala, S., Boniface, J., & Srikanth, V. V. S. S. (2014). Equilibrium and kinetics of Safranin O dye adsorption on MgO decked multi-layered graphene. *Chemical Engineering Journal, 258*, 412–419.

Roushani, M., Mavaei, M., & Rajabi, H. R. (2015). Graphene quantum dots as novel and green nano-materials for the visible-light-driven photocatalytic degradation of cationic dye. *Journal of Molecular Catalysis A: Chemical, 409*, 102–109.

Seema, H., Kemp, K. C., Chandra, V., & Kim, K. S. (2012). Graphene-SnO_2 composites for highly efficient photocatalytic degradation of methylene blue under sunlight. *Nanotechnology, 23*, 355705.

Sharma, P., & Das, M. R. (2013). Removal of a cationic dye from aqueous solution using graphene oxide nanosheets: investigation of adsorption parameters. *Journal of Chemical Engineering & Data, 58*(1), 151–158.

Sharma, P., Saikia, B. K., & Das, M. R. (2014). Removal of methyl green dye molecule from aqueous system using reduced graphene oxide as an efficient adsorbent: kinetics, isotherm and thermodynamic parameters. *Colloids and Surfaces A: Physicochemical and Engineering Aspects, 457*, 125–133.

Shen, J., Huang, W., Li, N., & Ye, M. (2015). Highly efficient degradation of dyes by reduced graphene oxide–ZnCdS supramolecular photocatalyst under visible light. *Ceramics International, 41*, 761–767.

Shi, P., Su, R., Wan, F., Zhu, M., Li, D., & Xu, S. (2012). Co_3O_4 nanocrystals on graphene oxide as a synergistic catalyst for degradation of orange II in water by advanced oxidation technology based on sulfate radicals. *Applied Catalysis B: Environmental, 123–124*, 265–272.

Siddhardha, R. S. S., Kumar, V. L., Kaniyoor, A., Muthukumar, V. S., Ramaprabhu, S., Podila, R., Rao, A. M., & Ramamurthy, S. S. (2014). Synthesis and characterization of gold graphene composite with dyes as model substrates for decolorization: a surfactant free laser ablation approach. *Spectrochimica Acta*

Part A: Molecular and Biomolecular Spectroscopy, 133, 365–371.

Singh, B. R., Shoeb, M., Khan, W., & Naqvi, A. H. (2015). Synthesis of graphene/zirconium oxide nanocompositephotocatalyst for the removal of rhodamineB dye from aqueous environment. *Journal of Alloys and Compounds, 651*, 598–607.

Sui, Z. Y., Cui, Y., Zhu, J. H., & Han, B. H. (2013). Preparation of three-dimensional graphene oxide−polyethylenimine porous materials as dye and gas adsorbents. *ACS Applied Materials & Interfaces, 5*(18), 9172–9179.

Sun, H., Cao, L., & Lu, L. (2011). Magnetite/reduced graphene oxide nanocomposites: one step solvothermal synthesis and use as a novel platform for removal of dye pollutants. *Nano Research, 4*(6), 550–562.

Sun, L., Yu, H., & Fugetsu, B. (2012). Graphene oxide adsorption enhanced by in situ reduction with sodium hydrosulfite to remove acridine orange from aqueous solution. *Journal of Hazardous Materials, 203–204*, 101–110.

Suresh, D., Nethravathi, P. C., Udayabhanu, Nagabhushana, H., & Sharma, S. C. (2015a). Spinach assisted green reduction of graphene oxide and its antioxidant and dye absorption properties. *Ceramics International, 41*(3) part B, 4810–4813.

Suresh, D., Udayabhanu, Kumar, M. A. P., Nagabhushana, H., & Sharma, S. C. (2015b). Cinnamon supported facile green reduction of graphene oxide, its dye elimination and antioxidant activities. *Materials Letters, 151*, 93–95.

Thangavel, S., Venugopal, G., & Kim, S. J. (2014). Enhanced photocatalytic efficacy of organic dyes using β-tin tungstatee reduced graphene oxide nanocomposites. *Materials Chemistry and Physics, 145*, 108–115.

Tiwari, J. N., Mahesh, K., Le, N. H., Kemp, K. C., Timilsina, R., Tiwari, R. N., & Kim, K. S. (2013). Reduced graphene oxide-based hydrogels for the efficient capture of dye pollutants from aqueous solutions. *Carbon, 56*, 173–182.

Torres, S. M., Pastrana-Martínez, L. M., Figueiredo, J. L., Faria, J. L., & Silva, A. M. T. (2013). Graphene oxide-P25 photocatalysts for degradation of diphenhydramine pharmaceutical and methyl orange dye. *Applied Surface Science, 275*, 361–368.

Ullah, K., Ye, S., Zhu, L., Meng, Z. D., Sarkar, S., & Oh, W. C. (2014). Microwave assisted synthesis of a noble metal-graphene hybrid photocatalyst for high efficient decomposition of organic dyes under visible light. *Materials Science and Engineering B, 180*, 20–26.

Vadivel, S., Vanitha, M., Muthukrishnaraj, A., & Balasubramanian, N. (2014). Graphene oxide–BiOBr composite material as highly efficient photocatalyst for degradation of methylene blue and rhodamine-B dyes. *Journal of Water Process Engineering, 1*, 17–26.

Vinothkannan, M., Karthikeyan, C., Kumar, G., Kim, A. R., & Yoo, D. J. (2015). One-pot green synthesis of reduced graphene oxide (RGO)/Fe3O4 nanocomposites and its catalytic activity toward methylene blue dye degradation. *Spectrochimica Acta Part A: Molecular and Biomolecular Spectroscopy, 136*(part B), 256–264.

Wang, J., Tsuzuki, T., Tang, B., Hou, X., Sun, L., & Wang, X. (2012). Reduced graphene oxide/ZnO composite: reusable adsorbent for pollutant management. *ACS Applied Materials & Interfaces, 4*(6), 3084–3090.

Wang, S., Wei, J., Lv, S., Guo, Z., & Jiang, F. (2013). Removal of organic dyes in environmental water onto magnetic-sulfonic graphene nanocomposite. *CLEAN–Soil, Air, Water, 41*(10), 992–1001.

Wang, X., Liu, Z., Ye, X., Hu, K., Zhong, H., Yu, J., Jin, M., & Guo, Z. (2014a). A facile one-step approach to functionalized graphene oxide-based hydrogels used as effective adsorbents toward anionic dyes. *Applied Surface Science, 308*, 82–90.

Wang, C., Zhu, J., Wu, X., Xu, H., Song, Y., Yan, J., Song, Y., Ji, H., Wang, K., & Li, H. (2014b). Photocatalytic degradation of bisphenol A and dye by graphene-oxide/Ag_3PO_4 composite under visible light irradiation. *Ceramics International, 40*(6), 8061–8070.

Wang, C., Cao, M., Wang, P., Ao, Y., Hou, J., & Qian, J. (2014c). Preparation of graphene–carbon nanotube–TiO2 composites with enhanced photocatalytic activity for the removal of dye and Cr (VI). *Applied Catalysis A: General, 473*, 83–89.

Wang, W., Cheng, Y., Kong, T., & Cheng, G. (2015a). Iron nanoparticles decoration onto three-dimensional graphene forrapid and efficient degradation of azo dye. *Journal of Hazardous Materials, 299*, 50–58.

Wang, Y., Pei, Y., Xiong, W., Liu, T., Li, J., Liu, S., & Li, B. (2015b). New photocatalyst based on graphene oxide/chitin for degradation of dyes under sunlight. *International Journal of Biological Macromolecules, 81*, 477–482.

Wang, L., Xin, X., Yang, M., Ma, X., Shen, J., Song, Z., & Yuan, S. (2015c). Effects of graphene oxide and salinity on sodium deoxycholate hydrogels and their applications in dye absorption. *Colloids and Surfaces A: Physicochemical and Engineering Aspects, 483*, 112–120.

Weber Jr., W. J., & Morris, J. C. (1963). Kinetics of adsorption on carbon from solution. *Journal of the Sanitary Engineering Divison, American Society of Civil Engineers, 89*, 31–60.

Wu, Q., Feng, C., Wang, C., & Wang, Z. (2013). A facile one-pot solvothermal method to produce superparamagnetic graphene–Fe_3O_4 nanocomposite and its application in the removal of dye from aqueous solution. *Colloids and Surfaces B: Biointerfaces, 101*, 210–214.

Yan, W. M., Huang, J. R., Tong, Z. W., Li, W. H., & Chen, J. (2013). Reduced graphene oxide–cuprous oxide composite via facial deposition for photocatalytic dye-degradation. *Journal of Alloys and Compounds, 568*, 26–35.

Yang, Y., Xie, Y., Pang, L., Li, M., Song, X., Wen, J., & Zhao, H. (2013a). Preparation of reduced graphene oxide/poly(acrylamide) nanocomposite and its adsorption of Pb(II) and methylene blue. *Langmuir, 29*(34), 10727–10736.

Yang, Z., Yan, H., Yang, H., Li, H., Li, A., & Cheng, R. (2013b). Flocculation performance and mechanism of graphene oxide for removal of various contaminants from water. *Water Rsesearch, 47*, 3037–3046.

Yao, Y., Xu, C., Yu, S., Zhang, D., & Wang, S. (2013). Facile synthesis of Mn_3O_4-reduced graphene oxide hybrids for catalytic decomposition of aqueous organics. *Industrial & Engineering Chemistry Research, 52*(10), 3637–3645.

Yoon, H. J., Choi, Y. I., Jang, E. S., & Sohn, Y. (2015). Graphene, charcoal, ZnO, and ZnS/BiOX (X = Cl, Br, and I) hybrid microspheres for photocatalytic simulated real mixed dye treatments. *Journal of Industrial and Engineering Chemistry, 32*, 137–152.

Yu, Y., Murthy, B. N., Shapter, J. G., Constantopoulos, K. T., Voelcker, N. H., & Ellis, A. V. (2013). Benzene carboxylic

acid derivatized graphene oxide nanosheets on natural zeolites as effective adsorbents for cationic dye removal. *Journal of Hazardous Materials, 260*, 330–338.

Zhang, L. L., Xiong, Z., & Zhao, X. S. (2010). Pillaring chemically exfoliated graphene oxide with carbon nanotubes for photocatalytic degradation of dyes under visible light irradiation. *ACS Nano, 4*(11), 7030–7036.

Zhang, Y., Chen, Z., Liu, S., & Xu, Y. J. (2013). Size effect induced activity enhancement and anti-photocorrosion of reduced graphene oxide/ZnO composites for degradation of organic dyes and reduction of Cr(VI) in water. *Applied Catalysis B: Environmental, 140–141*, 598–607.

Zhang, X., Yu, H., Yang, H., Wan, Y., Hu, H., Zhai, Z., & Qin, J. (2015). Graphene oxide caged in cellulose microbeads for removal of malachite green dye from aqueous solution. *Journal of Colloid and Interface Science, 437*, 277–282.

Zhao, G., Jiang, L., He, Y., Li, J., Dong, H., Wang, X., & Hu, W. (2011). Sulfonated graphene for persistent aromatic pollutant. *Advanced Materials, 23*(34), 3959–3963.

Zhao, F., Dong, B., Gao, R., Su, G., Liu, W., Shi, L., Xia, C., & Cao, L. (2015a). A three-dimensional graphene-TiO_2 nanotube nanocomposite with exceptional photocatalytic activity for dye degradation. *Applied Surface Science, 351*, 303–308.

Zhao, C., Guo, J., Yang, Q., Tong, L., Zhang, J., Zhang, J., Gong, C., Zhou, J., & Zhang, Z. (2015b). Preparation of magnetic Ni@graphene nanocomposites and efficient removal organic dye under assistance of ultrasound. *Applied Surface Science, 357*, 22–30.